High-frequency noise measurements in spin-valve devices

N. A. Stutzke
Boise State University, Boise, Idaho 83725

S. L. Burkett[a)]
University of Arkansas, Fayetteville, Arkansas 72701

S. E. Russek
National Institute of Standards and Technology, Boulder, Colorado 80305

(Received 15 October 2002; accepted 21 April 2003; published 30 June 2003)

High-frequency magnetic noise in magnetoresistive devices being developed for read-sensor and magnetic random access memory applications may present fundamental limitations on the performance of submicrometer magnetic devices. High-frequency magnetic noise (HFN) arises from intrinsic thermal fluctuations of the device magnetization. High-frequency noise spectroscopy provides a powerful tool to characterize the dynamics and response of small multilayer magnetic devices. In this study, the noise characteristics of micrometer-dimension spin valves have been investigated at frequencies in the range 0.1–6 GHz. At frequencies below this range $1/f$ noise dominates. HFN measurements, as a function of bias current and longitudinal magnetic field, are obtained for IrMn exchange-biased spin valves using a 50 GHz spectrum analyzer, low-noise amplifier, and a microwave probing system. The magnetic noise is obtained by taking the difference between the noise spectrum of the device in a saturated and unsaturated state. The data can be fit to simple models that predict the noise power to be proportional to the imaginary part of the free-layer magnetic susceptibility. There are some important differences between the high-frequency noise measurements and direct measurements of the device susceptibility (both at the device and wafer level). The noise measurements show a smaller damping parameter (a smaller ferromagnetic resonance linewidth) and additional features due to the presence of nonuniform modes. [DOI: 10.1116/1.1582458]

I. INTRODUCTION

Magnetoresistive devices are currently used in hard-disk read heads and are being developed for use in nonvolatile magnetic random-access memory. Performance of giant magnetoresistance (GMR) and tunneling magnetoresistance (TMR) devices in data storage applications is strongly dependent on the attainable signal-to-noise ratio. High-frequency magnetic noise (HFN) due to thermal magnetization fluctuations is inversely proportional to device volume. As device sizes shrink and operating frequencies approach the gigahertz range, high-frequency magnetic noise may limit performance.[1–4] Thermal magnetic noise as a function of bias current and longitudinal magnetic field in micrometer-size spin valves has been measured in the frequency range 0.1–6 GHz. Device noise spectra, showing both single and nonsingle domain behavior, will be presented.

The test system used in measuring high-frequency magnetic noise is shown in Fig. 1(a). Noise spectroscopy measurements were obtained by applying a dc bias current to the spin valve through a bias tee. The device, coupled through the capacitive port of the bias tee, is connected to a low noise amplifier, the output of which is sent to a 50 GHz spectrum analyzer interfaced to a computer. Contact to the spin valve was made via microwave probes to on-chip coplanar waveguides inside a variable temperature microwave probe station. Besides allowing the device temperature to be controlled, the chamber also provided shielding from external noise sources. Figure 1(b) shows a picture of the microwave probes contacting a device via a high-frequency coplanar waveguide.

The spin valves investigated consisted of Ta(5 nm)– $Ni_{0.8}Fe_{0.2}$ (5 nm)–$Co_{0.9}Fe_{0.1}$ (1 nm)–Cu(2.7 nm)–$Co_{0.9}Fe_{0.1}$ (2.5 nm)–Ru(0.6 nm)–$Co_{0.9}Fe_{0.1}$ (1.5 nm)–$Ir_{0.2}Mn_{0.8}$ (10 nm)–Ta(5 nm) multilayers sputtered on oxidized Si substrates. The GMR stack was deposited in a field of 15 mT to set the direction of the pinned layer. The blanket films used in fabricating the devices had a wafer level GMR ratio of 7.8%–8.1%. The wafer level response of one of the multilayers is shown in Fig. 2. After patterning, the devices typically had a GMR ratio of 5%, which is lower than the sheet level value primarily due to the lead and contact resistances. Data presented here were taken from rectangular devices patterned so that the pinned direction was perpendicular to the easy axis, which is the long axis of the rectangular device as shown in the bottom inset in Fig. 3. Device widths ranged from 0.6 to 1 μm, with aspect ratios of 2–4. Spin valves in two different contact configurations were investigated. The first type had overlayed contacts that overlapped the ends of the rectangular device, leaving only the portion of the device between them electrically active. The second had butted contacts that connected directly to the ends of the device. An atomic force microscope (AFM) image of a 0.8×3.8 μm^2 device with overlapping contacts is shown in the top inset in Fig. 3.

a)Electronic mail: sburkett@uark.edu

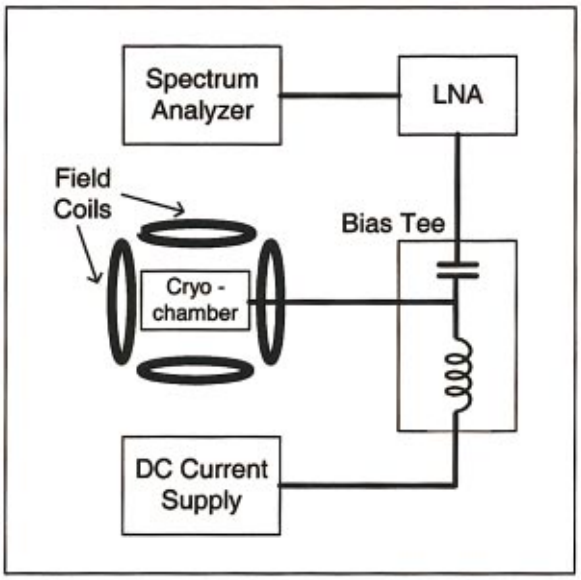

(a)

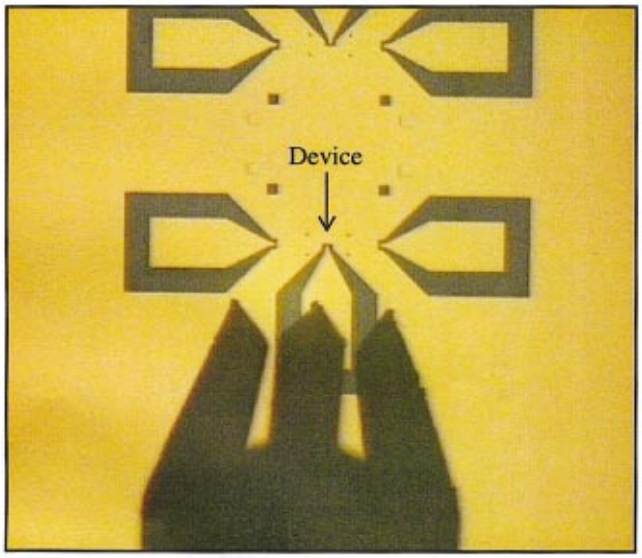

(b)

FIG. 1. (a) Diagram of the system used to measure high-frequency magnetic noise. (b) Image of microwave probes contacting a device.

Figure 3 shows a hard-axis magnetoresistance curve for an overlayed-contact device. For the butted contacts, the long ends of the rectangle under the two contacts are etched away and the GMR stack is present only in the gap between the leads.

II. EXPERIMENTAL PROCEDURE

The magnetic noise spectrum is obtained through a subtraction process as shown in Fig. 4. First a noise spectrum is collected with the device biased at the current and longitudinal magnetic field of interest. Then a reference spectrum is taken with the spin valve transversely saturated in a 14 mT externally applied hard axis field. In transverse saturation, small angle magnetic fluctuations in the free layer do not cause a change in resistance and therefore no voltage fluctuations will be measured by the spectrum analyzer. The difference between the two measured noise spectrums gives the noise due to thermal magnetization fluctuations. The noise spectra are then normalized by the amplifier gain and the square root of the spectrum analyzer bandwidth to obtain the device noise in volts per root hertz.

The majority of the data collected could be fit reasonably well using single-domain models that predict the noise power to be proportional to the imaginary part of the transverse magnetic susceptibility. The fluctuation-dissipation theorem[2,5] can be used to relate the noise spectra to the imaginary part of the transverse magnetic susceptibility (χ_t'') as

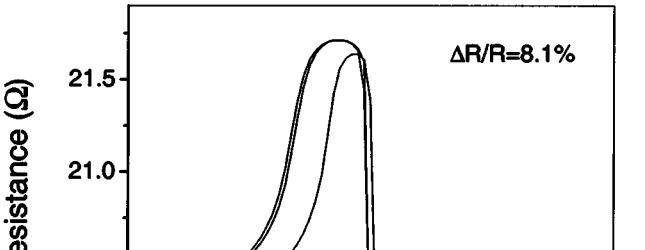

FIG. 2. Wafer-level magnetoresistance curve for multilayers used in the fabrication of butted-contact spin-valve devices.

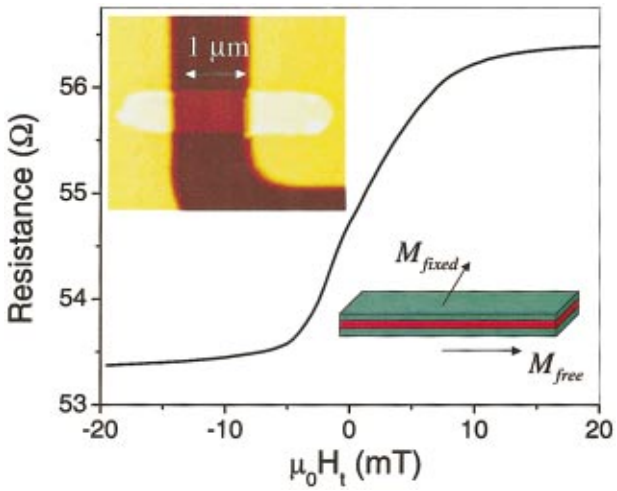

FIG. 3. Hard-axis magnetoresistance curve for a 0.8×3.7 μm^2 spin valve with overlapping contacts. The upper and lower insets show, respectively, an AFM image of a 0.8×3.7 μm^2 spin valve with overlapping contacts and a schematic of the magnetization orientations in zero field.

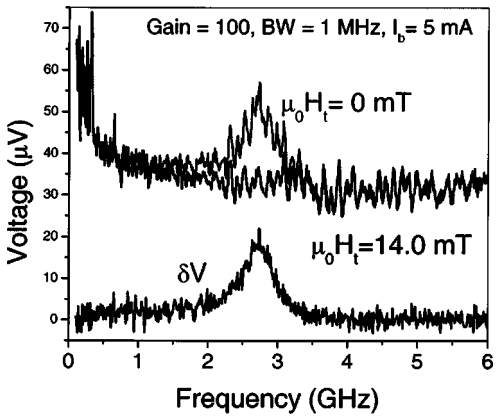

FIG. 4. Raw noise spectra taken with no transverse field and a large transverse field (sufficiently large so that the magnetization is saturated). The difference of these two voltage spectra is shown in the lower trace. The magnetic noise spectrum is obtained by normalizing the difference signal by the system gain and the square root of the system bandwidth (BW). The noise spectrum is further smoothed by adjacent point averaging.

$$V_n(f) = I\Delta R \sqrt{\frac{k_B T}{2\pi f \mu_0 M_s^2 V}\chi_t''(f)}, \tag{1}$$

where V_n is the voltage noise spectrum, I is the bias current, ΔR is the difference in device resistance between parallel and antiparallel states, T is the device temperature, M_s is the free layer saturation magnetization, V is the volume of the free layer, and f is the measurement frequency. The susceptibility, assuming single domain response, is given by

$$\chi_t''(f) = \frac{f}{\gamma'}\alpha\mu_0 M_s \times \left[\frac{\mu_0^2 M_s^2 + \frac{f^2}{\gamma'^2}}{\mu_0^2\left((H_k + H_l)M_s - \frac{f^2}{\gamma'^2}\right)^2 + \left(\frac{f}{\gamma'}\alpha\mu_0 M_s\right)^2}\right], \tag{2}$$

where γ' is the gyromagnetic ratio divided by 2π (28 GHz/T), H_k is the in-plane anisotropy field, H_l is the externally applied longitudinal field, and α is the Gilbert damping parameter. Fitting the data allowed for extraction of the magnetic damping parameter (which is proportional to the resonance linewidth), the in-plane anisotropy, and the ferromagnetic resonance (FMR) frequency. From Eqs. (1) and (2), the resonant frequency is

$$f_r \cong \gamma' \mu_0 \sqrt{(H_k + H_l)M_s} \tag{3}$$

and the voltage noise amplitude at the resonant peak is

$$V_n(f_r) \cong \frac{I\Delta R}{f_r}\sqrt{\frac{k_B T \gamma'}{2\pi\alpha M_s V}}\ . \tag{4}$$

We therefore expect that the resonant frequency will be proportional to the square root of the applied longitudinal field and the peak voltage noise will be inversely proportional to the resonant frequency. For more discussion of the fitting equations and the variation of the damping parameter see Ref. 6.

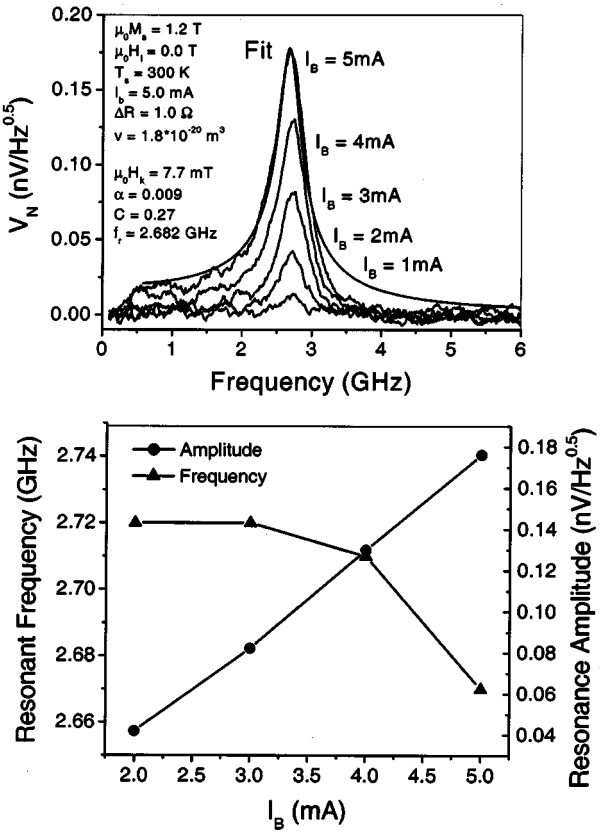

FIG. 5. (a) Magnetic noise spectra from a 1×3 μm^2 overlayed-contact spin-valve device taken at various bias currents. The fit to the 5 mA data is shown along with the input fitting parameters and the determined values of α, H_k, and f_r. (b) Resonant frequencies and maximum noise amplitudes obtained from fitting the data in (a). The resonant peak increases in amplitude and decreases in frequency with increasing bias current.

III. RESULTS

Noise spectra, measured at various bias currents on an overlayed-contact device with an active area of 1×2 μm^2, are shown in Fig. 5(a). Figure 5(b) shows a summary of the FMR amplitude and frequency as a function of bias current as obtained from fits to Eqs. (1) and (2). The device current, volume, longitudinal bias field, and saturated magnetization are taken from experiment and H_k, α, and an overall scale factor, C, are allowed to vary. An example fit is shown in the top plot of Fig. 5(a). H_k, which determines the resonant frequency, is 7.7 ± 0.1 mT and α, which determines the width of the peak, is 0.009 ± 0.001. The uncertainties in the anisotropy field and damping constant predominantly come from the uncertainty in the measured film magnetization ($\mu_0 M_s = 1.2\pm0.2$ T). The scale constant C, which determines the overall peak height, is 0.27, indicating that the data do not quantitatively agree with the noise amplitude predicted by Eqs. (1) and (2). Rather, the measured data are 0.27 times

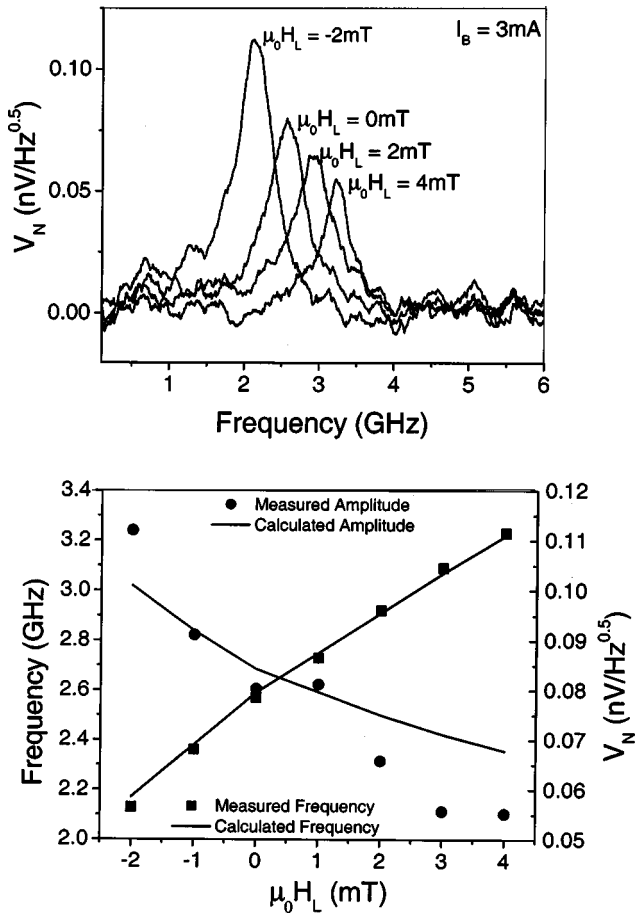

FIG. 6. (a) Series of magnetic noise spectra from a 1×3 μm^2 overlayed-contact spin-valve device taken at different longitudinal bias field. (b) Resonant frequencies and maximum noise amplitudes obtained from fitting the data in (a) and calculated values. Calculated values were obtained by using parameters from the $\mu_0 H_l = 0$ fit and inserting the applied field values into Eqs. (3) and (4).

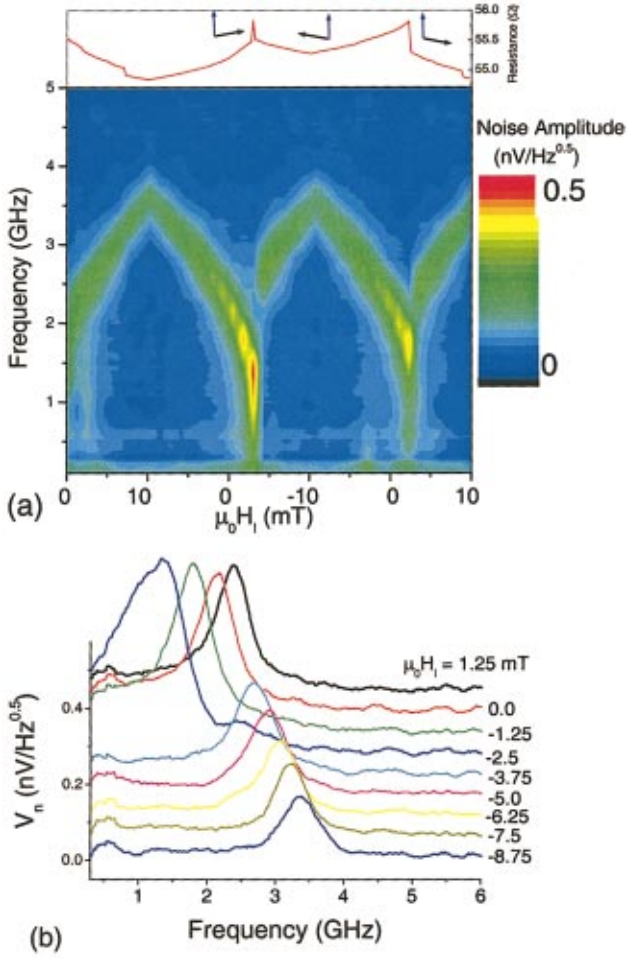

FIG. 7. (a) Two-dimensional plot of the noise spectra for a longitudinal field scan starting at 0 mT, going to 10 mT, back to -10 mT, and back to 0 mT. The plot at the top shows the magnetoresistance of the device taken concurrently with the noise data. The black and blue arrows schematically indicate the orientations of the free and fixed layer, respectively. The square-root dependence of the resonant frequency on longitudinal bias field is seen with the resonant frequency approaching zero near the switching field. (b) Noise spectra showing the region around the switching event at $\mu_0 H_l = 3.5$ mT. Near the switching threshold the resonant frequency approaches zero and the resonance width broadens.

that predicted. The experimental data are also seen to fall off more quickly at high frequencies than predicted by Eqs. (1) and (2).

As predicted by Eq. (1), the amplitude of the FMR peak increased linearly with bias current. For this device the amplitude of the resonant peak ranged from 0.04 to 0.18 nV/$\sqrt{\text{Hz}}$ as bias current was increased from 2 to 5 mA. A decrease of approximately 50 MHz was observed in the FMR frequency as the bias current was increased from 1 to 5 mA. The bias current creates hard-axis magnetic fields that slightly change the operating point and stiffness fields of the device. Direct measurement of the resonant frequency shift in a hard axis field gave a 110 MHz frequency shift for a 2.5 mT field. If we assume that only 60% of the current in the spin valve flows above the free layer (predominantly in the spacer layer and fixed magnetic layer) then a 5 mA bias current will generate a 1.8 mT hard axis field and give a predicted frequency shift of 47 MHz, which is close to the observed value. Other factors, such as device heating, which change M_s, will also contribute to the shift in resonance frequency with applied current bias.

Noise spectra of the above-mentioned device at a bias current of 3 mA for various longitudinal bias fields are shown in Fig. 6(a). Positive bias fields, which are in the same direction as the free layer magnetization, increase the stiffness field of the device. As longitudinal field is increased the FMR peak amplitude decreases and the FMR frequency increases. This behavior is similar to the results of standard FMR measurements on single layer films.[7] Increasing the longitudinal field by 6 mT resulted in an increase in resonant frequency just over 1 GHz and a decrease in peak amplitude from 0.115 to 0.055 nV/$\sqrt{\text{Hz}}$. Figure 6(b) summarizes the longitudinal field data and fits made to the noise spectra using Eqs. (1) and (2). The calculated values were found by using the parameters extracted from the $\mu_0 H_l = 0$ mT fit and inserting the applied field values into Eqs. (3) and (4). As seen in the figure, the resonant frequency change with longitudinal field is well predicted by the single domain model. However, the amplitude of the FMR peak decreases more

rapidly than expected as longitudinal bias field is increased. The higher than expected roll-off rate may be due to frequency dependent attenuation inherent to the measurement system. The frequency response of the entire system is currently under investigation.

Figure 7(a) shows a two-dimensional plot of the noise spectra as the longitudinal bias field is swept from 0 to 10 mT, to −10 mT, and finally back to 10 mT. The magnetoresistance, taken concurrently, is plotted above the noise spectra. The magnetoresistance shows that the device switches between its two easy-axis states at a field of approximately ±3.5 mT. Near the switching threshold, the resonant frequency approaches zero when $H_l = -H_k$ as predicted by Eq. (2). The resonant frequency does not go all the way to 0 since thermal fluctuations will cause the device to switch before the energy barrier goes to zero and the energy surface flattens. Figure 7(b) shows the noise spectra near the switching threshold. In addition to a lowering of the resonant frequency, the width of the resonance increases near the switching threshold ($\mu_0 H_l = -2.5$ mT).

Some devices showed nonsingle domain behavior as indicated by the presence of additional low-frequency noise peaks. One such example is shown in Fig. 8, which shows the magnetoresistance and noise spectra for a $0.6 \times 1.8\ \mu m^2$ butted-contact device measured at various transverse bias fields. For this device, micromagnetic structure is evident as shown by Barkhausen noise in the hard-axis magnetoresistance curves. As the micromagnetic state of the device changes, as indicated by the jumps in the MR curve, the low-frequency noise peaks shift in position and amplitude.

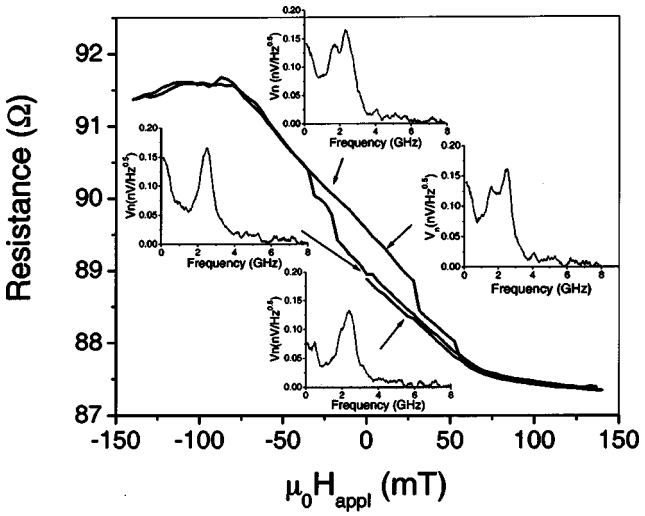

FIG. 8. Magnetoresistance and noise spectra for a $0.8 \times 1.6\ \mu m^2$ butted contact device. The magnetoresistance shows a series of hysteretic Barkhausen jumps indicating sudden changes in the micromagnetic structure of the device. The noise spectra, taken at several points along the magnetoresistance curve, show additional low-frequency peaks.

IV. SUMMARY

We have shown that high-frequency noise measurements are a useful method to characterize the dynamical structure of small multilayer GMR devices. Many devices have a noise spectrum that can be well fit with simple single domain models. The models accurately predict the observed shift in the resonance frequency and qualitatively describe the fall-off in noise amplitude as a function of longitudinal bias field. The shift in the resonant frequency with current bias is predominantly due to current-generated fields, and the frequency shift may be an accurate method to determine the internal fields in the device. Finally, the noise spectra can show fluctuation modes that arise due to micromagnetic structure in the devices and may be an important technique for investigating deviations from single-domain behavior.

[1]N. Smith and P. Arnett, Appl. Phys. Lett. **78**, 1448 (2001).
[2]N. Smith, J. Appl. Phys. **90**, 5768 (2001).
[3]J. C. Jury, K. B. Klaassen, J. C. L. van Peppen, and S. X. Wang, IEEE Trans. Magn. **38**, 3435 (2002).
[4]Z. Jin and H. N. Bertram, IEEE Trans. Magn. **38**, 2265 (2003).
[5]L. D. Landau and E. M. Lifshitz, *Statistical Physics* (Pergamon, New York, 1980), Chap. 12.
[6]N. A. Stutzke, S. L. Burkett, and S. E. Russek, Appl. Phys. Lett. **82**, 91 (2003).
[7]T. J. Silva, in *The Physics of Ultra High Density Recording*, edited by M. L. Plumer, J. Van Ek, and D. Weller (Springer, Berlin, 2001), pp. 110.